





Distribution of torsional stress between the un-replicated and replicated regions in partially replicated molecules

Víctor Martínez, Christian Schaerer, Pablo Hernández, Dora B. Krimer, Jorge B. Schwartzman & María-José Fernández-Nestosa

To cite this article: Víctor Martínez, Christian Schaerer, Pablo Hernández, Dora B. Krimer, Jorge B. Schwartzman & María-José Fernández-Nestosa (2020): Distribution of torsional stress between the un-replicated and replicated regions in partially replicated molecules, Journal of Biomolecular Structure and Dynamics, DOI: [10.1080/07391102.2020.1751294](https://doi.org/10.1080/07391102.2020.1751294)


To link to this article: <https://doi.org/10.1080/07391102.2020.1751294>

 View supplementary material [↗](#)

 Accepted author version posted online: 02 Apr 2020.
Published online: 10 Apr 2020.

 Submit your article to this journal [↗](#)

 Article views: 11

 View related articles [↗](#)

 View Crossmark data [↗](#)



Distribution of torsional stress between the un-replicated and replicated regions in partially replicated molecules

Víctor Martínez^a, Christian Schaerer^a, Pablo Hernández^b, Dora B. Krimer^b, Jorge B. Schwartzman^b and María-José Fernández-Nestosa^a

^aPolytechnic School, National University of Asunción, San Lorenzo, Paraguay; ^bDepartment of Cellular and Molecular Biology, Centro de Investigaciones Biológicas (CSIC), Madrid, Spain

Communicated by Ramaswamy H. Sarma

ABSTRACT

DNA topology changes continuously as replication proceeds. Unwinding of the DNA duplex by helicases is favored by negative supercoiling but it causes the progressive accumulation of positive supercoiling ahead of the fork. This torsional stress must be removed for the fork to keep advancing. Elimination of this positive torsional stress may be accomplished by topoisomerases acting solely ahead of the fork or simultaneously in the un-replicated and replicated regions after diffusion of some positive torsional strain from the un-replicated to the replicated regions by swivelling of the replication forks. In any case, once replication is completed fully replicated molecules are known to be heavily catenated and this catenation derives from pre-catenanes formed during replication. Although there is still controversy as to whether fork swivelling redistributes this positive torsional stress continuously or only as termination approaches, the forces that cause fork rotation and the generation of pre-catenanes are still poorly characterized. Here we used a numerical simulation, based on the worm-like chain model and the Metropolis Monte Carlo method, to study the interchange of supercoiling and pre-catenation in a naked circular DNA molecule of 4,440 bp partially replicated *in vivo* and *in vitro*. We propose that a dynamic gradient of torsional stress between the un-replicated and replicated regions drives fork swivelling allowing the interchange of supercoiling and pre-catenation.

ARTICLE HISTORY

Received 14 January 2020
Accepted 18 March 2020

KEYWORDS

DNA topology; replication; supercoiling; pre-catenation metropolis Monte Carlo


Introduction

DNA replication represents an important topological challenge. Due to the right-handed (RH) intertwined nature of the B-DNA double-helix, unwinding by DNA helicases causes a compensatory overwinding of the duplex ahead of the replication fork and this overwinding leads to positive (+) supercoiling (Kornberg & Baker, 1992). In bacterial cells negative (-) supercoiling facilitates the parental strands separation that is needed for the advance of DNA replication (Funnell et al., 1986; Marians et al., 1986; Martinez-Robles et al., 2009). The progressive accumulation of torsional stress in the form of (+) supercoiling immediately ahead of the fork would prevent its progression. During replication, elimination of this (+) supercoiling is accomplished by DNA topoisomerases acting solely ahead of the fork or simultaneously in the un-replicated and replicated regions after diffusion of the (+) supercoiling from the un-replicated to the replicated region by swivelling of the replication fork. In this way the un-replicated region remains always (-) supercoiled. This latter pathway, originally proposed by Champoux and Been (Champoux & Been, 1980), reduces the torsional stress immediately ahead of the replication fork at the expense of generating

(+) intertwined pre-catenanes in the replicated region (Champoux & Been, 1980; Ullsperger et al., 1995). It is important to notice that once replication is completed, fully replicated sister duplexes end-up (+) intertwined (Martinez-Robles et al., 2009; Sundin & Varshavsky, 1980, 1981).

Whether or not replication forks are able to rotate as they advance *in vivo* is still a matter of controversy (Cebrian et al., 2015; Mariezcurrena & Uhlmann, 2017; Schalbeter et al., 2015). In any case, after DNA isolation once all proteins are removed, *in vitro* the torsional stress of the un-replicated and replicated regions of a replication intermediate (RI) must equilibrate and this could only be accomplished by fork rotation (Schvartzman et al., 2019; Schvartzman & Stasiak, 2004). More specifically, in a free state, the system formed by both regions of the RI reaches thermodynamic equilibrium if the molecule is in mechanical equilibria, which in turn is achieved when the torque is balanced in the whole molecule. Winding or unwinding of the un-replicated portion of the plasmid applies torque to the replication forks, while braiding or unbraiding the replicated portion of DNA also applies torque to the forks but in the opposite direction, so that the net torque is cancelled in the equilibrium state.

CONTACT Jorge B. Schwartzman ✉ schvartzman@cib.csic.es Department of Cellular and Molecular Biology, Centro de Investigaciones Biológicas (CSIC), Ramiro de Maeztu 9, Madrid 28040, Spain; María-José Fernández-Nestosa ✉ mjfernandez@pol.una.py Polytechnic School, National University of Asunción, P.O. Box 2111, San Lorenzo, Paraguay.

 Supplemental data for this article can be accessed online at <https://doi.org/10.1080/07391102.2020.1751294>.

© 2020 Informa UK Limited, trading as Taylor & Francis Group

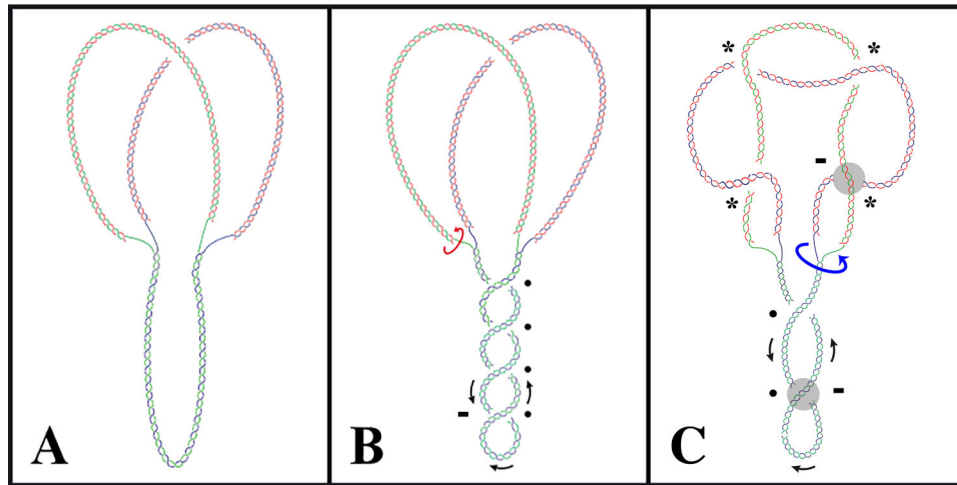


Figure 1. Cartoons illustrating the topology of partially replicated DNA molecules. (A): Fully relaxed replication intermediate. (B): Negatively supercoiled replication intermediate showing four (-) crossings in the un-replicated region (indicated by dots) and four (-) pre-catenane crossings (indicated by asterisks) in the replicated one. Note that the migration of each (-) crossing from the un-replicated region to the replicated one leads to two (-) crossings. Parental DNA duplex is depicted in blue and green whereas the sister duplexes of partially replicated molecules are depicted in blue and red and green and red, respectively, indicating that they are the natural products of replication where the newly synthesized strands are depicted in red.

Another consequence of mechanical equilibrium is that the potential energy gradient between the two regions must be null. Torsional stress generated by replisome progression should partition ahead of and behind the fork to maintain a balance of torque (Le et al., 2019). An important aspect to be considered, given the particular conformation of RIs, is the topological sign in the distribution of torsional stress between the replicated and un-replicated regions. The molecule represented in Figure 1A corresponds to a half-replicated fully relaxed form. Figure 1B represents a half-replicated molecule with (-) supercoiling in the un-replicated region and no pre-catenation in the replicated one. This is how half-replicated molecules would look *in vivo* if fork rotation was prevented except at termination (Schalbetter et al., 2015; Sundin & Varshavsky, 1980, 1981). After DNA isolation, fork rotation would allow redistribution of the torsional strain between the un-replicated and replicated regions. Once equilibrium is achieved, the supercoils in the un-replicated region would remain (-) and the sister duplexes in the replicated region would wind around each other in a (-) manner, too (Figure 1C). Note that the diffusion of each (-) supercoil crossing from the unreplicated region to the replicated one generates two (-) pre-catenane crossings (Champoux & Been, 1980; Schwartzman & Stasiak, 2004; Ullsperger et al., 1995).

Most studies on DNA topology are performed on bacterial circular plasmids that are closed topological domains. During replication these small circular DNA molecules remain (-) supercoiled. Understanding the interplay between supercoiling and pre-catenation in partially replicated molecules is hindered, though, by the fact that DNA conformation is disturbed during sample preparation. On the other hand, several studies convincingly proved that computer simulation can give a very accurate description of the DNA properties that are difficult to address experimentally (Martinez-Robles et al., 2009; Rawdon et al., 2016; Vologodskii, 2011; Vologodskii & Rybenkov, 2009; Vologodskii & Cozzarelli, 1993;

Witz & Stasiak, 2010). For all these reasons, here we used the worm-like chain (WLC) model in combination with Metropolis Monte Carlo (MC) numerical simulation to study the dynamics of DNA topology in partially replicated plasmid DNA molecules, once these RIs are isolated *in vitro*. In the WLC model the DNA is represented as a chain of rigid cylinders of equal length, whose conformation can be described as a simple set of parameters: bending elasticity, torsional rigidity and effective double-helix diameter (Racko et al., 2017; Vologodskii, 1992; Vologodskii & Rybenkov, 2009; Vologodskii & Cozzarelli, 1993).

The topological and energetic characterization of circular DNA plasmids depends on the Linking number (Lk), which is an integer that measures the winding of the two strands of the double helix around each other and is unaffected by changes in the conformation of the DNA, as long as these do not involve the breakage of one or both strands. Lk is a topological invariant established by the Calugareanu-White-Fuller relation, $Lk = Wr + Tw$ (Fuller, 1971), where Tw (Twist) determines the degree of torsional deformation of the double helix and Wr (Writhe) is a number that describes the three-dimensional folding of the molecule (Klenin & Langowski, 2000). The torsional stress in a topologically closed DNA molecule can be expressed in terms of the linking number difference, $\Delta Lk = Lk - Lk_0$, where Lk_0 is the Lk for relaxed DNA. The topology of partially replicated plasmids also depends on the pre-catenation number that describes the interlinking between the two sister duplexes and equals half of the signed sum of intermolecular nodes (Sundin & Varshavsky, 1980, 1981). For replication intermediates isolated *in vitro* ΔLk should be distributed both ahead and behind the replication fork (Peter et al., 1998; Schwartzman et al., 2019; Schwartzman et al., 2013; Ullsperger et al., 1995). Multiple catenated DNA duplexes result after nicking and religation (Vologodskii & Cozzarelli, 1993; Wasserman et al., 1988). The ΔLk observed is a result of the

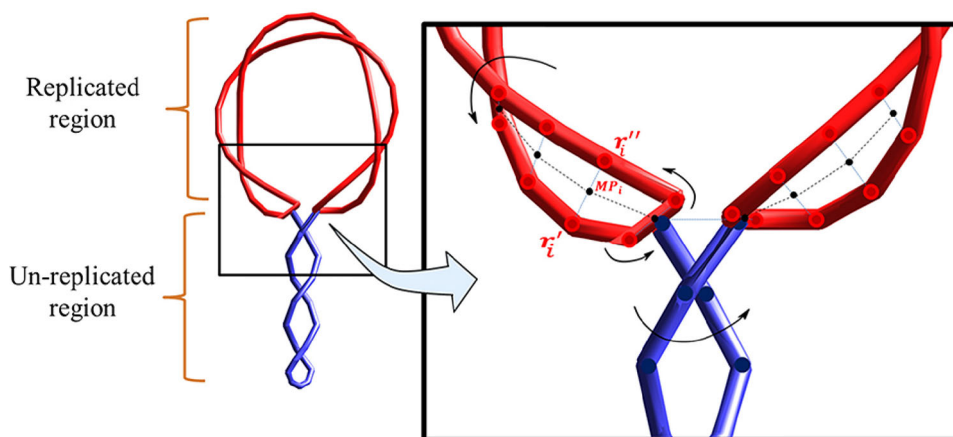


Figure 2. Simulation of fork rotation in partially replicated DNA molecules. Modeled replication intermediate (RI). Newly replicated sister DNA molecules multiply interlinked with (-) pre-catenane crossings (in red) and the un-replicated supercoiled region with (-) plectonemes (in blue). The mechanism to model fork rotation is shown in the inset figure. Opposite points of the replicated curves, r'_i and r''_i , located on each curve are rotated with respect to their midpoint MP_i over the same angle. Braiding or unbraiding of the replicated curves results from the contribution of rotations of all the pair of points of these curves. The topology of the un-replicated region is modified only by the effect of Metropolis MC method.

writhe induced by catenation. When catenated DNA molecules are supercoiled their extent of supercoiling is expressed by the effective ΔLk (ΔLk_e), which is defined as the difference between the actual Lk and the equilibrium linking number for the given catenated rings or knotted DNA molecule (Burnier et al., 2008; Schwartzman et al., 2019). In the case of RIs, the replicated region could also acquire a ΔLk that is induced by the inter-duplex crossings of the sister duplexes.

To understand the conformational properties of partially replicated DNA molecules in thermodynamic equilibrium, we used a mathematical approach, based on numerical simulations of RIs with the forks stalled at different sites before termination and without any mechanical impediment that avoids the propagation of torsional stress between both regions of the molecule through the replication forks (in a free state, after deproteinization). In each case, we generated a WLC ensemble of RIs with a certain degree of torsional strain accumulated either ahead or behind the forks, causing a non-vanishing torque. Replication forks were allowed to rotate until the torque balance was achieved, changing the distribution of the elastic energy between the replicated and un-replicated regions in order to find the thermodynamic equilibrium conformation using the Metropolis MC procedure. Our results confirmed a dynamic interchange of torsional stress between the two regions separated by the forks. The equilibrium distribution of torsional stress is related to the location of the replication forks relative to the termination sites.

Material and methods

The replication intermediate model

We modeled double-stranded DNA as a discrete worm-like chain (Frank-Kamenetskii et al., 1985; Vologodskii & Cozzarelli, 1993; Vologodskii et al., 1992). In this model DNA is represented by a series of rigid segments that are cylinders of constant length (3.4 nm) and thickness (3.0 nm), according to the value of the DNA effective diameter, impenetrable to each other. To model RIs using the WLC we created an un-

replicated region connected through replication forks to two circular molecules representing the sister duplexes of the replicated region. We modeled a circular plasmid DNA of 4440 bp where 25, 50 or 75% of the molecule has been replicated. In the case of the 50% replicated molecules, the un-replicated region as well as each nascent duplex in the replicated region were composed of 200 segments (2220 bp). In the case of 25% and 75% replicated molecules, the number of segments in each simulated curve was proportional to the length in bp of the simulated regions of the RI.

Figure 2 shows a half replicated molecule with DNA strands of the un-replicated and replicated parts modeled as a single and double coupled WLC, respectively. The un-replicated region (in blue) is connected through replication forks to two circular molecules representing the sister duplexes of the replicated region (in red). Newly replicated sister DNA duplexes could be multiply interlinked with (-) pre-catenanes and un-replicated DNA is (-) supercoiled. The topology of the RIs was modified by winding/unwinding the plectonemic structure of the un-replicated region or by braiding/unbraiding both nascent curves in the replicated portion. The number of supercoil crossings in the un-replicated region and the number of pre-catenane crossings in the replicated one determines the ΔLk of the RI. The mechanism to model replication forks rotation is shown in the inset of Figure 2. Red and blue dots represent the junction between consecutive segments while black dots correspond to the midpoints of the central axis between the red curves. Fork swiveling was achieved through rotation of both red curves around each other. In geometric terms, this was accomplished by applying the rotation of the two opposite points r'_i and r''_i (in each red curve) with respect to their midpoint MP_i . The segment $r'_i - MP_i - r''_i$ was rotated over an angle φ from its original orientation maintaining the point MP_i fixed. Depending on the direction, the rotation resulted in braiding or unbraiding of newly replicated curves, changing the topology of the replicated region. Through this mechanism, both forks were able to rotate at every step of the simulation procedure.

Energy fundamentals

The elastic potential energy model considered for simulated DNA molecules included the bending elastic energy, denoted by E_b , and the torsional energy, denoted by E_t (Vologodskii et al., 1992). Considering the WLC model, the bending energy is given by

$$E_b = k_B T \alpha \sum_{i=1}^N \theta_{i,i+1}^2, \quad (1)$$

where N denotes the number of segments, $\theta_{i,i+1}$ is the angular displacement between two consecutive segments, i and $i+1$, k_B is the Boltzmann constant, T is the absolute temperature (297 K), and α is the bending rigidity constant (Frank-Kamenetskii et al., 1985; Vologodskii & Cozzarelli, 1993; Vologodskii et al., 1992).

The torsional energy depends on the displacement of chain twist from its equilibrium value, ΔTw , and in this model it can be expressed by the equation $\Delta Tw = \Delta Lk - Wr$ (de Vries, 2005; Fuller, 1971), where ΔLk is the linking number difference of the simulated DNA. The value of ΔLk is considered as a constant parameter at each iteration of the simulation procedure (Vologodskii et al., 1992) and the Wr is a function of a single space curve that is necessary to compute after each trial move of the Metropolis MC method. Hence, the torsional energy E_t is defined as

$$E_t = \frac{2\pi^2 C}{L} \Delta Tw^2 = \frac{2\pi^2 C}{L} (\Delta Lk - Wr)^2, \quad (2)$$

where C is the torsion rigidity constant of the molecule ($4.50 \cdot 10^{-19}$ J.bp) and L is the DNA length expressed in bp (Vologodskii & Cozzarelli, 1993). Super-helical stress was relaxed in the nascent chains due to the single-stranded breaks. For this reason, the only component of the total energy of the replicated curves was the bending energy E_b .

Simulation procedure and computational performance

Using the model described above we created three curves, one that represents the un-replicated region and the other two corresponding to the nascent duplexes of the replicated region. The length of every curve was related to the percentage of replication that was simulated (25, 50 or 75%). The Metropolis MC procedure was applied to find the minimum elastic energy conformation and trial perturbations consisted in the rotation of an arbitrary number of adjacent segments of the WLC ensemble by a random angle around the straight line connecting two randomly chosen fixed points (Frank-Kamenetskii et al., 1985; Vologodskii & Cozzarelli, 1993; Vologodskii et al., 1992). The total number of turns of the replication forks, $Total_{Turns}$, and the total number of steps of the simulation, $Total_{Steps}$, determined the value of the rotation angle of the replication forks at every step, $\sigma = 2\pi \frac{Total_{Turns}}{Total_{Steps}}$. Hence, the number of turns at every step of the simulation procedure is given by $\sigma/2\pi$.

For every simulation, a set of initial conformations was created, each with a specific value of ΔLk distributed between the un-replicated and replicated parts. The basic

step of the simulation procedure for the redistribution of the ΔLk between the two regions of the RI was accomplished by changing the supercoiling of the un-replicated region in a value $\sigma/2\pi$ and rotating the replicated curves around each other with the angle σ . The algorithm was set so that the braiding of the replicated curves caused a loss of supercoils in the un-replicated region, and vice-versa, in order to keep a constant value of ΔLk . Finally, the Metropolis MC method was applied to the entire molecule in order to find the minimum elastic energy conformation in which the net torque is vanished. This basic step was repeated to reach a selected complexity or a specific energetic property.

Results

Simulation of the interchange of supercoiling and pre-catenation in replicating DNA

To study the interchange of torsional strain between both regions in half replicated DNA molecules in deproteinized conditions *in vitro*, we performed numerical simulations using the WLC model and the Metropolis MC method to analyze the elastic potential energy of 50% replicated RIs by migrating all torsional stress from one region to the other. First, we modeled RIs with 10 (-) supercoil crossings and devoid of pre-catenane crossings. The parental strands in the un-replicated region were topologically constrained due to supercoiling, whereas in the replicated region the sister duplexes were relaxed because swiveling of the free ends of newly synthesized chains allows the release of any super-helical stress. This is how half-replicated molecules would look *in vivo* if fork rotation was prevented except at termination (Schalbetter et al., 2015; Sundin & Varshavsky, 1980, 1981). Once all proteins are removed *in vitro*, the local torsional stress accumulated could migrate from the un-replicated to the replicated region and vice-versa by swiveling of the replication forks. In this way the supercoiling of the un-replicated region could lead to intertwining of the daughter DNA duplexes. The forks were rotated to allow the migration of all the (-) crossings from the un-replicated region to the replicated one. Figure 3A shows the energy shift after each rotation as a function of the crossing numbers of the replicated and un-replicated regions. It is clearly noted that the value of elastic energy of DNA supercoiling in the un-replicated region (in blue) decreased as the pre-catenation number of the replicated DNA increased (in red). The average elastic potential energy (calculated from 10 independent simulations) of the initial conformation was 34.2 Kcal/mol, 29.6 Kcal/mol for the un-replicated region and 4.7 Kcal/mol for the replicated portion. At the end, the elastic energy of the un-replicated region was reduced to 4.2 Kcal/mol while the elastic energy of the replicated region increased to 46.6 Kcal/mol. An example of the simulations performed is shown in Supplementary Video 1.

We also modeled half-replicated RIs with 20 (-) crossings in the replicated region and devoid of crossings in the un-replicated region. In this case, swiveling of replication fork induced the migration of all torsional stress to the un-replicated region. The initial values of elastic energy, resulting

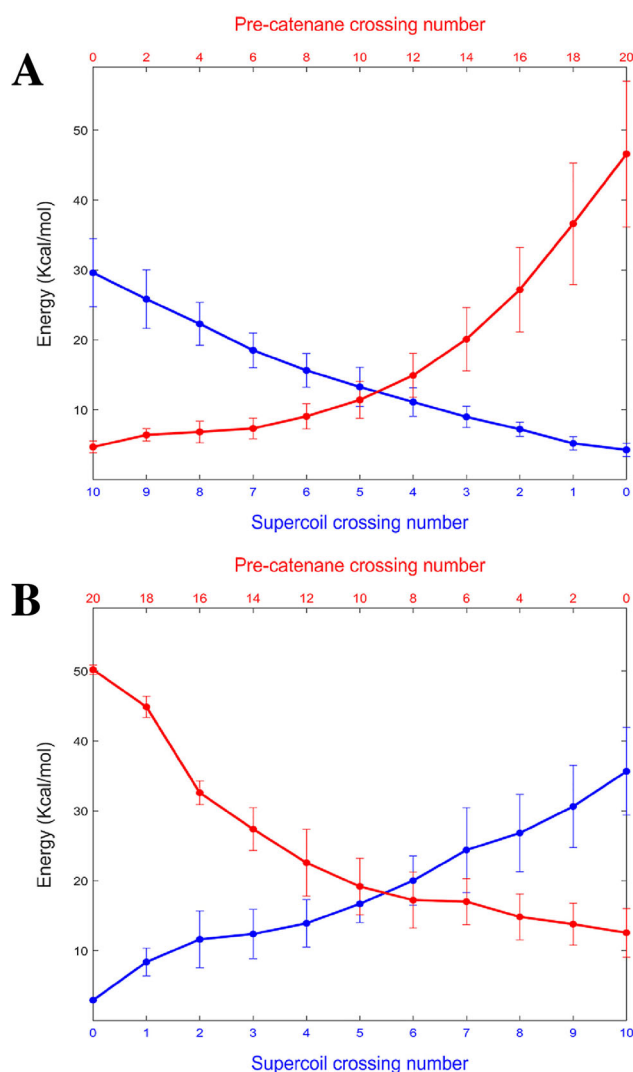


Figure 3. Fork rotation and migration of negative torsional stress between un-replicated and replicated regions. The topology of the RIs was modified through fork rotation either by changing the supercoiling of the un-replicated region or by rotating both nascent curves around each other in the replicated portion. Elastic energy was calculated after each rotation. (A): Profile of elastic energy corresponding to 50% replicated RIs with 10 (-) supercoil crossings in the un-replicated region and devoid of pre-catenanes. Forks were rotated to allow migration of all the (-) crossings from the un-replicated region to the replicated region. (B): Half replicated molecules with 20 (-) crossings in the replicated region and devoid of crossings in the un-replicated portion. Forks were rotated to allow the migration of all the (-) crossings from the replicated to the un-replicated region. Average values of elastic energy for the un-replicated (blue lines) and replicated (red lines) regions correspond to 10 independent simulations.

from 10 independent simulations, were 2.9 and 50.2 Kcal/mol for the un-replicated and replicated regions, respectively. The forks were rotated to allow the migration of all the (-) crossings from the replicated region to the un-replicated one. Figure 3B shows the energy shift after each rotation as a function of the crossing numbers of the replicated and un-replicated regions. It is clearly noted that here the value of elastic energy of pre-catenanes in the replicated region (in red) decreased as supercoiling in the un-replicated region increased (in blue). At the end, the elastic energy of the replicated region was reduced to 12.6 Kcal/mol while the elastic energy of the replicated region increased to 35.6 Kcal/mol. These results confirmed that our model for a RI *in vitro*

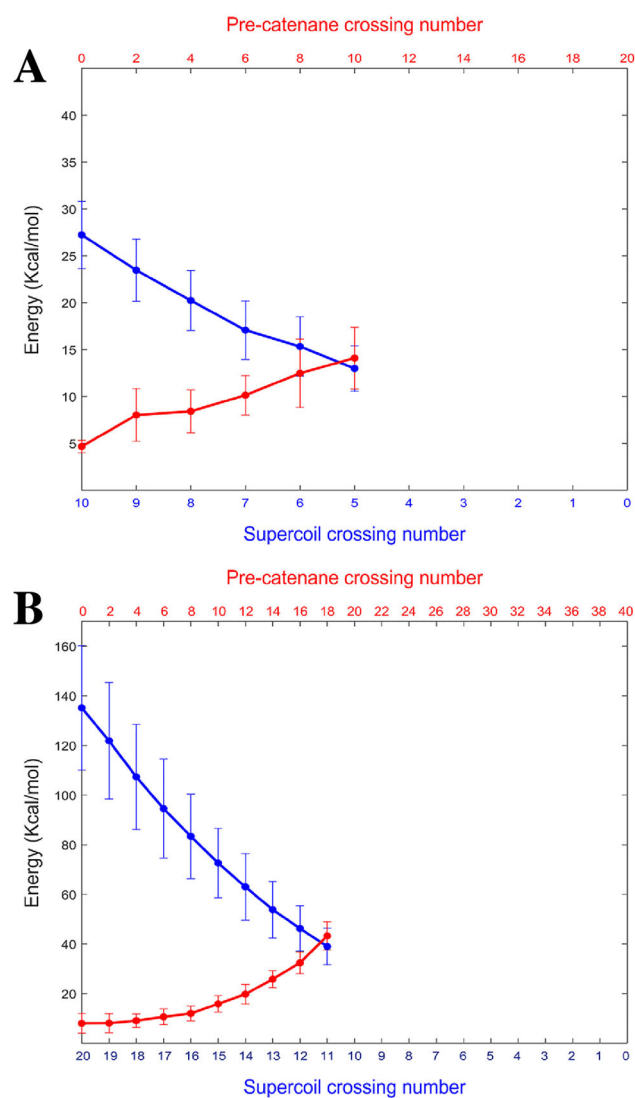


Figure 4. Thermodynamic equilibrium of 50% replicated negatively supercoiled DNA molecules. Swiveling of the replication fork allowed migration of torsional stress until both regions reached thermodynamic equilibrium. (A): Distribution of elastic energy in 50% replicated RIs with 10 (-) supercoil crossings in the un-replicated region and devoid of pre-catenanes. (B): Half-replicated molecules with 20 (-) supercoil crossings in the un-replicated region and devoid of pre-catenanes. Average values of elastic energy, corresponding to 10 independent simulations. Un-replicated (blue lines) and replicated (red lines) regions are represented as a function of the supercoil and pre-catenane crossing numbers.

was able to reproduce the migration of torsional strain from the un-replicated to the replicated region and vice-versa. An example of the simulations performed is shown in [Supplementary Video 2](#).

Equilibrium conformation of half-replicated DNA molecules

In order to study the thermodynamic and conformational properties of the RIs in deproteinized conditions, we considered an ensemble of WLC-generated 50% replicated RIs with torsional strain accumulated either in the replicated or un-replicated region. In this case, swiveling of the replication forks allowed the migration of torsional stress until both regions reached thermodynamic equilibrium, i.e. the conformation in which the net torque of the molecule is vanished so the RI is in

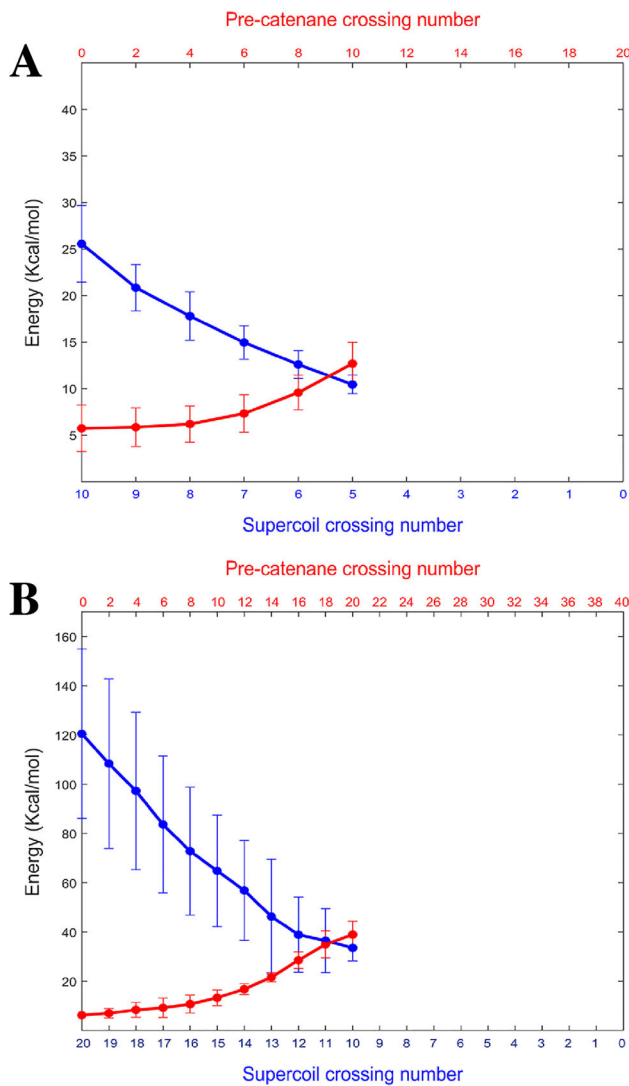


Figure 5. Thermodynamic equilibrium of 50% replicated positively supercoiled DNA molecules. Braiding of the replicated chains allowed the partial relaxation of (+) supercoils in the un-replicated region to achieve torque balance. (A): Distribution of elastic energy in 50% replicated RIs with 10 (+) supercoil crossings in the un-replicated region and devoid of pre-catenanes. (B): Half-replicated molecules with 20 (+) supercoil crossings in the un-replicated region and devoid of pre-catenanes. Average values of elastic energy, corresponding to 10 independent simulations, for the un-replicated (blue lines) and replicated (red lines) regions are represented as a function of the supercoil and pre-catenane crossing numbers.

mechanical equilibria. We modeled RIs with 10 (-) supercoils in the un-replicated region and devoid of pre-catenanes. Swiveling of the replication forks allowed partial release of the elastic energy accumulated in the un-replicated region to reach thermodynamic equilibrium (Supplementary Video 3). The elastic energy of both regions as a function of crossing numbers is shown in Figure 4A. In the initial conformation the values of energy were 27.2 and 4.7 Kcal/mol for the un-replicated and replicated regions, respectively. At thermodynamic equilibrium, the final value of energy was 13.7 Kcal/mol for each region. Under this condition, partially replicated molecules with supercoiling in the un-replicated region and devoid of pre-catenanes reached thermodynamic equilibrium by migrating half of the crossings of the un-replicated region to form the same number of pre-catenanes. The equilibrium conformation, resulting from 10 independent simulations,

corresponded to a RI with 5.3 (-) crossings in the un-replicated region and 4.7 (-) pre-catenanes.

To expand this analysis, we repeated the simulation procedure with half replicated RIs showing 20 (-) supercoils in the un-replicated region and devoid of pre-catenanes. As in the previous case, swiveling of the replication fork allowed a partial release of the torsional stress stored in the un-replicated region to reach thermodynamic equilibrium (Supplementary Video 4). The elastic energy of both regions as a function of crossing numbers is shown in Figure 4B. In the initial conformation the values of energy were 135.2 and 8.0 Kcal/mol for the un-replicated and replicated regions, respectively. At thermodynamic equilibrium the final value of potential elastic energy was 40.7 Kcal/mol for each region. Under this condition, partially replicated molecules with supercoiling in the un-replicated region and devoid of pre-catenanes reached thermodynamic equilibrium by migrating almost half of the crossings of the un-replicated region to form approximately the same number of pre-catenanes. The conformation with null net torque of the replication forks, resulting from 10 independent simulations, corresponded to a RI with 11.2 (-) crossings in the un-replicated region and 8.8 (-) pre-catenanes.

As previously mentioned, during DNA replication *in vivo*, unwinding of the parental DNA double-helix by DNA helicases causes a compensatory overwinding of the duplex ahead of the replication fork and this overwinding leads to positive (+) supercoiling (Kornberg & Baker, 1992). In 1980, Champoux and Been (Champoux & Been, 1980) proposed that in addition to the action of DNA topoisomerases in the un-replicated region, swiveling of the forks could reduce the (+) torsional tension accumulated immediately ahead of the replication fork at the expense of generating (+) intertwined pre-catenanes in the replicated region (Champoux & Been, 1980; Ullsperger et al., 1995). Therefore, to complete our analysis next we modeled RIs with 10 (+) supercoil crossings in the un-replicated region and devoid of pre-catenane crossings. Here, the parental strands in the un-replicated region were topologically constrained due to (+) supercoiling. Swiveling of the replication forks allowed partial release of the torsional stress accumulated in the un-replicated region to reach thermodynamic equilibrium (Supplementary Video 5). The elastic energy of both regions as a function of crossing numbers is shown in Figure 5A. In the initial conformation the values of energy were 25.6 and 5.7 Kcal/mol for the un-replicated and replicated regions, respectively. At thermodynamic equilibrium, the final value of energy was 11.4 Kcal/mol for each region. Under this condition, partially replicated molecules with (+) supercoiling in the un-replicated region and devoid of pre-catenanes reached thermodynamic equilibrium by migrating half of the crossings of the un-replicated region to form the same number of (+) pre-catenanes. The equilibrium conformation, resulting from 10 independent simulations, corresponded to a RI with 5.4 (+) crossings in the un-replicated region and 4.6 (+) pre-catenanes.

We repeated the simulation procedure with half replicated RIs showing 20 (+) supercoils in the un-replicated region and devoid of pre-catenanes. As in the previous case, swiveling of the replication fork allowed a partial release of the torsional

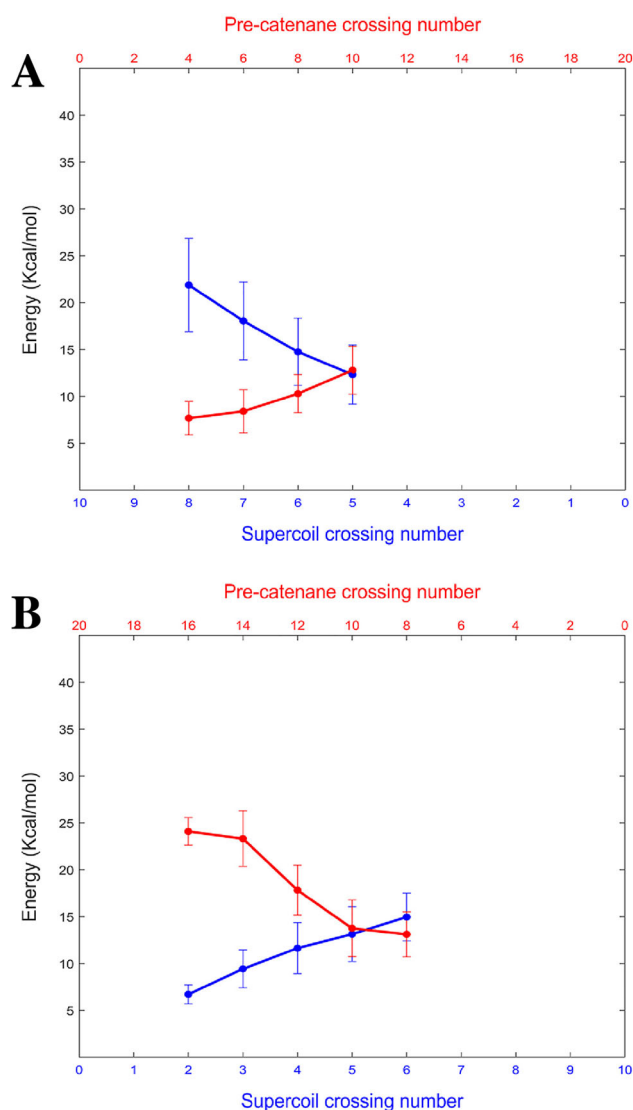


Figure 6. Distribution of torsional stress in 50% replicated RIs with different levels of topological complexity in the replicated and un-replicated regions. (A): Profiles of elastic energy corresponding to RIs with 8 (-) supercoil crossings in the un-replicated region and 4 (-) pre-catenane crossings in the replicated region. (B): RIs with 2 (-) supercoil crossings in the un-replicated region and 16 (-) pre-catenane crossings in the replicated portion. The replication forks were allowed to rotate until both regions reached thermodynamic equilibrium. Average values of elastic energy for the un-replicated (blue lines) and replicated (red lines) regions correspond to 10 independent simulations.

strain stored in the un-replicated region to reach thermodynamic equilibrium (Supplementary Video 6). The elastic energy of both regions as a function of crossing numbers is shown in Figure 5B. In the initial conformation the values of energy were 120.5 and 6.2 Kcal/mol for the un-replicated and replicated regions, respectively. At thermodynamic equilibrium the final value of energy was 35.8 Kcal/mol for each region. Under this condition, partially replicated molecules with (+) supercoiling in the un-replicated region and devoid of pre-catenanes reached thermodynamic equilibrium by migrating almost half of the crossings of the un-replicated region to form approximately the same number of (+) pre-catenanes. The equilibrium conformation, resulting from 10 independent simulations, corresponded to a RI with 10.8 (+) crossings in the un-replicated region and 9.2 (+) pre-catenanes.

Next we extended our analyses to show the distribution of mechanical stress in half-replicated RIs with different number of crossings in the un-replicated and replicated regions. In the first case, the initial conformation was a RI with 8 (-) supercoils in the un-replicated region and 2 (-) pre-catenanes in the replicated region. Rotation of the replication forks allowed the migration of torsional stress to balance the torque between both regions (Supplementary Video 7). The elastic energy as a function of the crossing numbers in both regions is shown in Figure 6A. There was a gradual loss of crossings in the un-replicated region with a synchronized acquisition of new intertwining between the two daughter duplexes. The initial values of elastic energy for the un-replicated and replicated regions were 21.9 and 7.7 Kcal/mol, respectively. Fork rotation stopped when both regions achieved the same elastic energy (12.6 Kcal/mol). The equilibrium conformation corresponded to a RI with 5.1 (-) supercoils and 4.9 (-) pre-catenanes. In the opposite situation, an ensemble of RIs with 2 (-) crossings in the un-replicated region and 16 (-) crossings in the replicated region, redistribution of torsional stress resulted in an equilibrium conformation with 5.3 (-) supercoils and 4.7 (-) pre-catenanes (Figure 6B). The initial values of energy of the un-replicated and replicated regions were 6.7 and 24.1 Kcal/mol, respectively. Total elastic potential energy at the equilibrium conformation was 27.2 Kcal/mol, 13.6 Kcal/mol for each region (Supplementary Video 8). These results confirmed that, for all the initial conformations tested, rotation of the replication forks to reach thermodynamic equilibrium allows a homogeneous distribution of torsional stress in 50% replicated molecules.

Distribution of the elastic energy of RIs with the forks stalled at different sites before termination

We further tested our model by probing an ensemble of RIs with different relative sizes of replicated and un-replicated regions. Inspired by *in vivo* experiments (Cebrian et al., 2015), we analyzed the distribution of elastic energy in a 25% replicated RI with 10 (-) supercoils in the un-replicated region and devoid of pre-catenanes. Fork rotation allowed the migration of torsional stress to reach thermodynamic equilibrium. The energy shift after each rotation of the forks is shown in Figure 7A. In the initial conformation, the elastic energy of the replicated region was 6.1 Kcal/mol and it was increased to 12.5 Kcal/mol at the equilibrium conformation. In the un-replicated region, there was a coordinated decline of energy from 21.1 to 12.5 Kcal/mol. The conformation in which the net torque is vanished, resulting from 10 independent simulations, corresponded to a RI with 6.8 (-) crossings in the un-replicated region and 3.2 (-) pre-catenanes in the replicated part. An example of the redistribution of torsional stress is shown in Supplementary Video 9.

Simulation was also used to analyze 75% replicated RIs with 10 (-) supercoils in the un-replicated region and devoid of crossings in the replicated region. Distribution of torsional stress by rotation of the replication forks to achieve torque balance occurred in such a way that most of the (-)

supercoils switched to (-) pre-catenanes. A profile of the elastic energy in both regions is shown in Figure 7B. Fork rotation stopped when both regions achieved thermodynamic equilibrium (15.6 Kcal/mol). The equilibrium conformation, resulting from 10 independent simulations, corresponded to a RI with 3.5 (-) crossings in the un-replicated region and 6.5 (-) pre-catenanes in the replicated region (Supplementary Video 10). These results demonstrated that the equilibrium distribution of torsional stress between both regions is related to the ratio between the sizes of both regions.

Figure 8 summarizes the initial and final conformations of some simulated cases (see also Supplementary Table 1). Altogether, these results showed that the equilibrium conformation is dynamic as it changes according to relative sizes of the replicated and un-replicated portions of the RI. For all the cases studied, the initial energy observed was greater than the final one when RIs reached thermodynamic equilibrium.

Discussion

Once replication terminates the newly synthesized sister duplexes appear heavily intertwined (Liu et al., 2009; Martinez-Robles et al., 2009; Schalbetter et al., 2015; Sundin & Varshavsky, 1980, 1981). Although DNA rings may be catenated *in vitro* (Baldi et al., 1980; Kreuzer & Cozzarelli, 1980), it was clearly shown that *in vivo* catenanes derive from pre-catenanes formed during replication (Adams et al., 1992; Martinez-Robles et al., 2009; Peter et al., 1998; Ullsperger et al., 1995). In turn, these pre-catenanes are formed due to the diffusion of torsional stress from the un-replicated to the replicated region of partially replicated molecules driven by fork swiveling (Cebrian et al., 2015; Champoux & Been, 1980; Ullsperger et al., 1995). By making direct torque measurements it was found that in naked DNA (without nucleosomes), torsional stress generated by replication is partitioned primarily behind the replisome. In contrast, in eukaryotes, a single chromatin fiber (like the un-replicated region) is torsionally soft and a braided fiber (like the replicated chains) is torsionally stiff, meaning that the superhelical stress on chromatin is preferentially stored in the un-replicated region (Le et al., 2019). However, when and how do replication forks rotate to allow the passage of torsional stress from the un-replicated to the replicated region is still poorly understood.

A very important aspect to be considered is the topological sign of supercoiling in the un-replicated region and pre-catenation in the replicated one. In all the cases studied so far *in vivo*, catenane's crossings in fully replicated sister duplexes are (+) (Sundin & Varshavsky, 1980, 1981). As these catenanes derive from pre-catenanes, their crossings should be (+) as well. We previously discussed that *in vivo*, pre-catenation forms due to the diffusion of torsional stress from the un-replicated to the replicated regions of partially replicated molecules facilitated by fork swiveling (Cebrian et al., 2015; Champoux & Been, 1980; Ullsperger et al., 1995). Therefore, we must conclude that the (+) pre-catenanes formed *in vivo* derive from (+) supercoiling that transiently

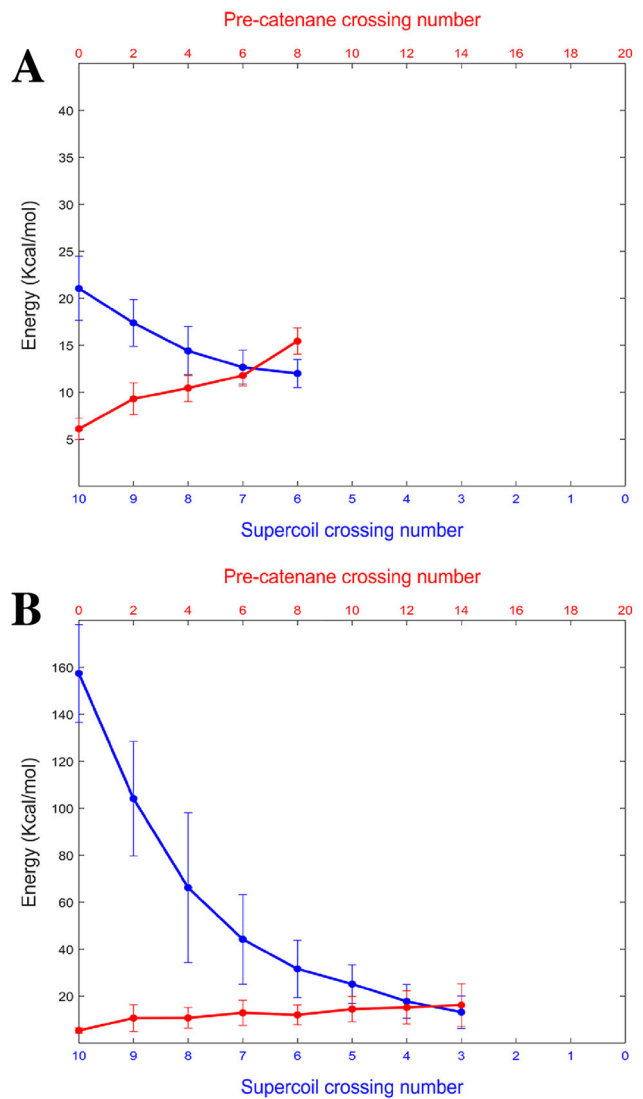


Figure 7. Distribution of torsional stress in 25 and 75% replicated negatively supercoiled DNA molecules. (A): Profiles of elastic energy as a function of the crossing numbers corresponding to 25% replicated RI, with 10 (-) supercoils in the un-replicated region and devoid of pre-catenanes. (B): 75% replicated RI, with 10 (-) supercoil crossings in the un-replicated region and devoid of pre-catenanes. Average values of elastic energy for the un-replicated (blue lines) and replicated (red lines) correspond to 10 independent simulations.

accumulate immediately ahead of progressing forks. In prokaryotes, topoisomerase IV (Topo IV) is ~ 20 times more efficient eliminating (+) than (-) crossings (Crisona et al., 2000; Stone et al., 2003). It was also shown that bacterial plasmids are more torsionally tensioned in the absence of Topo IV (Cebrian et al., 2015). These observations indicate that in bacterial plasmids interconversion of (+) supercoiling from the un-replicated region and pre-catenane's (+) crossings occurs continuously during replication. On the other hand, in the budding yeast, Schalbetter and co-workers showed that fork rotation and the formation of pre-catenanes during replication *in vivo* are actively inhibited by Timeless/Tof1 and Tipin/Csm3 and only occur in hard-to-replicate contexts such as stable protein-DNA fragile sites and termination (Schalbetter et al., 2015). In any case, during DNA isolation once all proteins are removed the replication forks of partially replicated molecules can rotate freely and the only force driving this

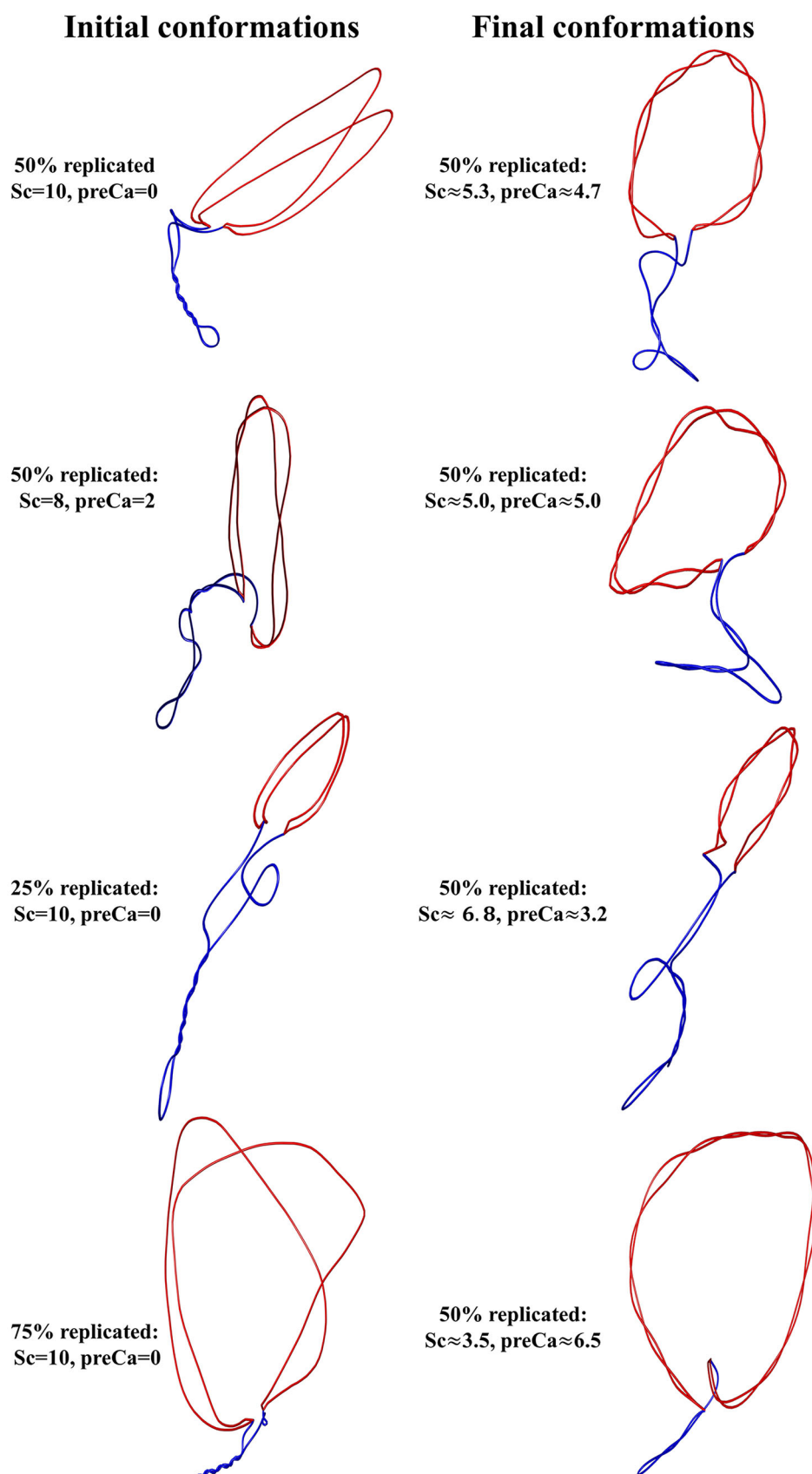


Figure 8. The initial and final conformations in several of the simulations tested. For a 50% replicated RI starting with 10 (-) supercoil crossings in the un-replicated region and devoid of pre-catenanes. For a 50% replicated RI starting with 8 (-) supercoil crossings in the un-replicated region and 4 (-) pre-catenane crossings in the replicated region. For a 25% replicated RI starting with 10 (-) supercoil crossings in the un-replicated region and devoid of pre-catenanes. And for a 75% replicated RI starting with 10 (-) supercoil crossings in the un-replicated region and devoid of pre-catenanes. In all cases the simulation procedure was stopped once thermodynamic equilibrium was achieved.

swiveling is the energy accumulated by torsional stress in the un-replicated and replicated regions. Taking this into account, here we developed a worm-like chain model to study the interchange of supercoiling and pre-catenation in partially replicated molecules in a deproteinized condition. Our study showed that, at thermodynamic equilibrium, torsional stress distribution depends on the progression of the replication fork, as seen for 25, 50 and 75% partially replicated molecules. We observed that the torsional stress accumulated in the un-replicated and replicated regions depends on their relative sizes, i.e. the extent of replication. These results confirmed that the equilibrium distribution of ΔLk between replicated and un-replicated regions should approximate to the ratio of their length in base pairs (Ullsperger et al., 1995). If the forks were only allowed to rotate as termination approaches most of the replicon would have already been replicated. On the contrary, if forks are allowed to swivel continuously, interchange of supercoils and pre-catenanes would continuously change as replication advances. This would certainly add another twist to the dynamics of DNA replication.

To our knowledge, this is the first study of the interchange of torsional strain between the un-replicated and replicated regions in replicating DNA using a numerical approach. In our numerical simulations, the energy gradient between both regions was significantly high at the beginning, when all the torsional stress was accumulated in one region (replicated or un-replicated). Once rotation of the replication fork was performed to achieve torque balance, the elastic energy difference between both regions was reduced as the torsional stress migrated from the region with higher complexity to the more relaxed one. The rate of change of the energy gradient between both regions of the RI was faster at the beginning and gradually slowed down as the RI approached to thermodynamic equilibrium. The imbalance in torque, as a consequence of the imposed local torsional strain, could be considered as the driving force of fork's rotation as it regulates the speed of the process. Here we propose that the distribution of torsional stress between the un-replicated and replicated regions drives fork swiveling allowing the interchange of supercoiling and pre-catenation during DNA replication.

Our model mimics partially replicated DNA strands with replication forks stalled at different sites before termination in deproteinized conditions. DNA strands of replicated and un-replicated regions were modeled as a single and double coupled WLC, respectively, separated by swiveling forks. To study the dynamic of the distribution of torsional strain between the two regions separated by the forks, we found the thermodynamic equilibrium conformation using Metropolis MC. The data obtained revealed that the equilibrium conformational properties of the simulated RIs were independent of the initial conditions or the topological sign of supercoiling (Figures 4–6).

The model proposed here assumes that in order to study the exchange between supercoiling and pre-catenation, we need to consider bending and torsional components of the elastic energy. DNA subjected to bending energy is often described by WLC modeling. This bending energy is faithfully

taken into by equation (1). On the other hand, simple WLC do not explicitly include twist degrees freedom. In the worm-like chain model, the elementary rods that form the simulated molecule of DNA usually have two degrees of freedom; bending and twisting. Twisting degree of freedom is associated with the rotation of one rod of the WLC respect to the next one. Bending degree of freedom is related to the angle between the axis of one rod respect to the axis of the adjacent rod (de Vries, 2005; Vologodskii et al., 1992). There are different approaches to calculate the torsional component of energy, including the twistable worm-like chain (TWLC) (Nomidis et al., 2019) or helical worm-like chain (Liu et al., 2011). Since we are not interested in the local twisting dynamics, or in the inhomogeneities of the distribution of the twist along the chain, the integration of the local twist angles along the chain can be used to define the torsional component of the elastic energy (de Vries, 2005). Here we used the expression of twist energy proposed by Vologodskii and co-workers (Vologodskii et al., 1992) that, despite its simplicity, describes many thermodynamic properties of DNA. This implementation of the WLC model has several assumptions and approximations, i.e. the approximation of the DNA as an isotropic elastic chain, so local sequence-dependent variations in structure are ignored; no consideration of supercoiling-driven structural transitions such as the introduction of cruciforms and Z-DNA; assumption that torsional and bending rigidity are independent; approximation of electrostatic interactions between DNA segments by cylinders whose effective diameter accounts for excluded volume effects (Vologodskii et al., 1992). Despite of these limitations, the simulation procedure used here reproduces physical properties of supercoiled and catenated DNA (Martinez-Robles et al., 2009; Vologodskii & Cozzarelli, 1993; Vologodskii et al., 1992), referring specifically to the conformational properties of the un-replicated and replicated regions.

The Metropolis Monte Carlo method implemented in this study finds the potential elastic energy for each portion of the RI, which depends on the distribution of the elastic deformation between both regions. In all cases where the simulation procedure was stopped when both regions reached thermodynamic equilibrium there was a difference in total elastic energy between the initial and final conformations because the energy profiles presented do not include other components of total energy, like the kinetic energy or the dissipated energy. Such difference was more evident in molecules accumulating more torsional stress, like the one shown in Figure 4B ($\Delta Lk = -20$). In the case of the 75% replicated molecule (Figure 7B & Supplementary Video 10), the size of the un-replicated region is significantly shorter and the bending effect is greater. As a consequence, the initial energy was higher than that for 50% replicated molecules, which in turn was higher than the initial energy of 25% replicated RIs. Independently of the relative size of both regions, the final conformations had similar elastic energy values. In the case where the final energy was greater than the initial one (Figure 3A & Supplementary Video 1) the difference observed was due to the simulation procedure resulting in a final conformation that could not have been

reached through a spontaneous process. Nonetheless, it was of interest to study the energy properties at this state, too.

Another theoretical approximation for numerical simulations of replication intermediates could be tested in future works with a model that includes more degrees of freedom than those exposed in the model implemented here, i.e. models in which local variations of the torsion angles are taken into account. Alternatively, as a future task, computational methods such as molecular dynamics (MD) simulations could be used to predict replication fork dynamics and the evolution of the simulated molecules through the phase space.

Disclosure statement

No potential conflict of interest was reported by the author(s).

Funding

This work was sustained by grant PINV15-573 from the Paraguayan CONACYT-PROCIENCIA program to MJFN and BFU2014-56835 from the Spanish Ministerio de Economía y Competitividad to JBS. The authors acknowledge the critics and continuous support of Prof. Andrzej Stasiak.

References

- Adams, D. E., Shekhtman, E. M., Zechiedrich, E. L., Schmid, M. B., & Cozzarelli, N. R. (1992). The role of topoisomerase-IV in partitioning bacterial replicons and the structure of catenated intermediates in DNA replication. *Cell*, *71*(2), 277–288. doi:10.1016/0092-8674(92)90356-H
- Baldi, M. I., Benedetti, P., Mattoccia, E., & Tocchini-Valentini, G. P. (1980). In vitro catenation and decatenation of DNA and a novel eucaryotic ATP-dependent topoisomerase. *Cell*, *20*(2), 461–467. doi:10.1016/0092-8674(80)90632-7
- Burnier, Y., Dorier, J., & Stasiak, A. (2008). DNA supercoiling inhibits DNA knotting. *Nucleic Acids Research*, *36*(15), 4956–4963. doi:10.1093/nar/gkn467
- Cebrian, J., Castan, A., Martinez, V., Kadomatsu-Hermosa, M. J., Parra, C., Fernandez-Nestosa, M. J., Schaerer, C., Hernandez, P., Krimer, D. B., & Schwartzman, J. B. (2015). Direct evidence for the formation of precatenanes during DNA replication. *Journal of Biological Chemistry*, *290*(22), 13725–13735. doi:10.1074/jbc.M115.642272
- Champoux, J. J., & Been, M. D. (1980). Topoisomerases and the swivel problem. In B. Alberts (Ed.), *Mechanistic studies of DNA replication and genetic recombination* (pp. 809–815). Academic Press.
- Crisona, N. J., Strick, T. R., Bensimon, D., Croquette, V., & Cozzarelli, N. R. (2000). Preferential relaxation of positively supercoiled DNA by E. coli topoisomerase IV in single-molecule and ensemble measurements. *Genes & Development*, *14*(22), 2881–2892. doi:10.1101/gad.838900
- de Vries, R. (2005). Evaluating changes of writhe in computer simulations of supercoiled DNA. *Journal of Chemical Physics*, *122*(6), 064905. doi:10.1063/1.1846052
- Frank-Kamenetskii, M. D., Lukashin, A. V., Anshelevich, V. V., & Vologodskii, A. V. (1985). Torsional and bending rigidity of the double helix from data on small DNA rings. *Journal of Biomolecular Structure and Dynamics*, *2*(5), 1005–1012. doi:10.1080/07391102.1985.10507616
- Fuller, F. B. (1971). The writhing number of a space curve. *Proceedings of the National Academy of Sciences of Sciences*, *68*(4), 815–819. doi:10.1073/pnas.68.4.815
- Funnell, B. E., Baker, T. A., & Kornberg, A. (1986). Complete enzymatic replication of plasmids containing the origin of the Escherichia coli chromosome. *The Journal of Biological Chemistry*, *261*(12), 5616–5624.
- Klenin, K., & Langowski, J. (2000). Computation of writhe in modeling of supercoiled DNA. *Biopolymers*, *54*(5), 307–317. doi:10.1002/1097-0282(20001015)54:5<307::AID-BIP20>3.0.CO;2-Y
- Kornberg, A., & Baker, T. A. (1992). *DNA replication* (2nd ed.). W.H. Freeman and Co.
- Kreuzer, K. N., & Cozzarelli, N. R. (1980). Formation and resolution of DNA catenanes by DNA gyrase. *Cell*, *20*(1), 245–254. doi:10.1016/0092-8674(80)90252-4
- Le, T. T., Gao, X., Park, S. H., Lee, J., Inman, J. T., Lee, J. H., Killian, J. L., Badman, R. P., Berger, J. M., & Wang, M. D. (2019). Synergistic coordination of chromatin torsional mechanics and topoisomerase activity. *Cell*, *179*(3), 619–631. doi:10.1016/j.cell.2019.09.034
- Liu, Z., Deibler, R. W., Chan, H. S., & Zechiedrich, L. (2009). The why and how of DNA unlinking. *Nucleic Acids Research*, *37*(3), 661–671. doi:10.1093/nar/gkp041
- Liu, Y., Perez, T., Li, W., Gunton, J. D., & Green, A. (2011). Statistical mechanics of helical wormlike chain model. *Journal of Chemical Physics*, *134*(6), 065107. doi:10.1063/1.3548885
- Marians, K. J., Minden, J. S., & Parada, C. (1986). Replication of superhelical DNAs in vitro. *Prog Nucleic Acids Res Mol Biol*, *33*, 111–140.
- Mariezcurrera, A., & Uhlmann, F. (2017). Observation of DNA intertwining along authentic budding yeast chromosomes. *Genes & Development*, *31*(21), 2151–2161. doi:10.1101/gad.305557.117
- Martinez-Robles, M. L., Witz, G., Hernandez, P., Schwartzman, J. B., Stasiak, A., & Krimer, D. B. (2009). Interplay of DNA supercoiling and catenation during the segregation of sister duplexes. *Nucleic Acids Research*, *37*(15), 5126–5137. doi:10.1093/nar/gkp530
- Nomidis, S. K., Skoruppa, E., Carlon, E., & Marko, J. F. (2019). Twist-bend coupling and the statistical mechanics of the twistable wormlike-chain model of DNA: Perturbation theory and beyond. *Physical Review E*, *99*(3-1), 032414doi:10.1103/PhysRevE.99.032414
- Peter, B. J., Ullsperger, C., Hiasa, H., Marians, K. J., & Cozzarelli, N. R. (1998). The structure of supercoiled intermediates in DNA replication. *Cell*, *94*(6), 819–827. doi:10.1016/S0092-8674(00)81740-7
- Racko, D., Benedetti, F., Dorier, J., Burnier, Y., & Stasiak, A. (2017). Molecular dynamics simulation of supercoiled, knotted, and catenated DNA molecules, including modeling of action of DNA gyrase. *Methods in Molecular Biology*, *1624*, 339–372. doi:10.1007/978-1-4939-7098-8_24
- Rawdon, E. J., Dorier, J., Racko, D., Millett, K. C., & Stasiak, A. (2016). How topoisomerase IV can efficiently unknot and decatenate negatively supercoiled DNA molecules without causing their torsional relaxation. *Nucleic Acids Research*, *44*(10), 4528–4538. doi:10.1093/nar/gkw311
- Schalbetter, S. A., Mansoubi, S., Chambers, A. L., Downs, J. A., & Baxter, J. (2015). Fork rotation and DNA precatenation are restricted during DNA replication to prevent chromosomal instability. *Proceedings of the National Academy of Sciences*, *112*(33), E4565–4570. doi:10.1073/pnas.1505356112
- Schwartzman, J. B., Hernandez, P., Krimer, D. B., Dorier, J., & Stasiak, A. (2019). Closing the DNA replication cycle: From simple circular molecules to supercoiled and knotted DNA catenanes. *Nucleic Acids Research*, *47*(14), 7182–7198. doi:10.1093/nar/gkz586
- Schwartzman, J. B., Martinez-Robles, M. L., Hernandez, P., & Krimer, D. B. (2013). The benefit of DNA supercoiling during replication. *Biochemical Society Transactions*, *41*(2), 646–651. doi:10.1042/BST20120281
- Schwartzman, J. B., & Stasiak, A. (2004). A topological view of the replicon. *EMBO Reports*, *5*(3), 256–261. doi:10.1038/sj.embor.7400101
- Stone, M. D., Bryant, Z., Crisona, N. J., Smith, S. B., Vologodskii, A., Bustamante, C., & Cozzarelli, N. R. (2003). Chirality sensing by Escherichia coli topoisomerase IV and the mechanism of type II topoisomerases. *Proceedings of the National Academy of Sciences*, *100*(15), 8654–8659. doi:10.1073/pnas.1133178100
- Sundin, O., & Varshavsky, A. (1980). Terminal stages of SV40 DNA replication proceed via multiply intertwined catenated dimers. *Cell*, *21*(1), 103–114. doi:10.1016/0092-8674(80)90118-X
- Sundin, O., & Varshavsky, A. (1981). Arrest of segregation leads to accumulation of highly intertwined catenated dimers dissection of the final stages of SV40 DNA replication. *Cell*, *25*(3), 659–669. doi:10.1016/0092-8674(81)90173-2
- Ullsperger, C., Vologodskii, A. A., & Cozzarelli, N. R. (1995). Unlinking of DNA by topoisomerases during DNA replication. In D. M. J. Lilley & F.

- Eckstein (Eds.), *Nucleic acids and molecular biology* (pp. 115–142). Springer-Verlag.
- Vologodskii, A. (1992). *Topology and physics of circular DNA*. CRC Press.
- Vologodskii, A. (2011). Unlinking of supercoiled DNA catenanes by type IIA topoisomerases. *Biophysical Journal*, 101(6), 1403–1411. doi:10.1016/j.bpj.2011.08.011
- Vologodskii, A. V., & Cozzarelli, N. R. (1993). Monte Carlo analysis of the conformation of DNA catenanes. *Journal of Molecular Biology*, 232(4), 1130–1140. doi:10.1006/jmbi.1993.1465
- Vologodskii, A. V., Levene, S. D., Klenin, K. V., Frank-Kamenetskii, M., & Cozzarelli, N. R. (1992). Conformational and thermodynamic properties of supercoiled DNA. *Journal of Molecular Biology*, 227(4), 1224–1243. doi:10.1016/0022-2836(92)90533-P
- Vologodskii, A., & Rybenkov, V. V. (2009). Simulation of DNA catenanes. *Physical Chemistry Chemical Physics*, 11(45), 10543–10552. doi:10.1039/b910812b
- Wasserman, S. A., White, J. H., & Cozzarelli, N. R. (1988). The helical repeat of double-stranded DNA varies as a function of catenation and supercoiling. *Nature*, 334(6181), 448–450. doi:10.1038/334448a0
- Witz, G., & Stasiak, A. (2010). DNA supercoiling and its role in DNA decatenation and unknotting. *Nucleic Acids Research*, 38(7), 2119–2133. doi:10.1093/nar/gkp1161